A Dynamic Analysis of Non-Uniform Microstrip Multi-Conductor Transmission Lines Using The Grounded Slab Green's Functions Approach

[1] Tawfik R. Arabi, [2] Arthur T. Murphy,
[3] Tapan K. Sarkar, & [3] Roger F. Harrington

[1] Intel Corporation, Architecture Development Lab
Department of Interconnect Technology Development

Abstract

The objective of this paper is to present a numerical technique based on a combined approach of using a "quasi-dynamic", a "dynamic" and an asymptotic approach for the analysis of non-uniform microstrip transmission lines and discontinuities using the grounded dielectric slab Green's Functions. The regions of validity of several quasi-dynamic and asymptotic approximations have been compared and determined in terms of the required accuracy and the microstrip physical parameters. Finally, numerical examples have been solved and checked with available and data and measurement in order to check the accuracy of this new technique.

1 Introduction

This paper describes an Electric Field Integral Equation Formulation (EFIEF) for the dynamic characterization of non-uniform microstrip transmission lines and discontinuities. In the dynamic approach, the green's functions $G_1(\rho)$ and $G_2(\rho)$ are Sommerfeld type integrals that can be evaluated only numerically. The crucial element to a numerical advantage of the EFIEF therefore, lies in the efficient computation of the green's functions, particularly in the analysis of electrically large structures. In this paper, a quasi dynamic approximation [1] has been used for the near field and an asymptotic steepest descent approximation for the far field calculations. The regions of validity of several quasi-dynamic and asymptotic approximations have been compared and determined in terms of the microstrip physical parameters and the required accuracy.

[1]The authors are with [2] DuPont Electronics, E.I. DuPont De Nemours & Co., Experimental Station, Wilmington, DE, 19880., [3] The Dept. of Electrical Engineering at Syracuse University, Syracuse, N.Y. 13244.

[2]This work was supported in part by a research grant from E. I. DuPont De Nemours & Company, and by grant for supercomputer time from the Cornell National Science Foundation SuperComputing Facility.

2 Moment Method Formulation

For the most general planar structures, the current distribution is a two dimensional current with both longitudinal and transversal flows [1]. For most transmission lines like structures however, the transversal current is negligible and thus the current may be assumed to flow in the axial direction only [1]. Such an assumption leads to a considerably more efficient moment method solution as it substantially reduces the generalized impedance matrix size. In this paper, a longitudinal current flow has been assumed. For the single microstrip line, the transversal component of the longitudinal flow has an analytical form that depends on $(\frac{W}{H})$ [1, 2, 3]. For a multi-conductor line (Fig. 1.) however, the transversal current distribution on each of the lines can no longer be approximated by a square root or a constant distribution due to the edge effects. The transversal distribution also depends on the location and number of the excited lines. In this paper, the transversal current distribution is obtained by solving the equivalent 2D problem involving the charge distribution [4,5]. The equivalence of the charge and current distributions for the uniform, infinite length, multi-conductor transmission line has been shown in [4].

2.1 Numerical Evaluation of The Green's Functions

In the dynamic approach, the Sommerfeld type Green's functions of the problem are evaluated exactly. The poles of the integrands have to be evaluated very accurately [6,7]. In this paper, we use a combined (iterative, Newton-Raphson) search, guaranteed to converge to any desired accuracy to determine the location of these poles. In this procedure, the error after the N^{th} iteration is bound by

$$error \leq \frac{z_{max} - z_{min}}{2^N} \quad (1)$$

Once the number and locations of the poles are determined, the Green's functions of the microstrip can then be easily numerically calculated using a strait forward guassian quadrature. The detailed procedure has been outlined in [1,8].

AA

CH3141-9/92/0000-1111$01.00 © 1992 IEEE

2.1.1 The Quasi-Dynamic Approximation

In this paper, the quasi-dynamic approximations G_{1q} and G_{2q} are defined as

$$G_{1q}(\rho) = \lim_{k_1 \longrightarrow 0} G_1(\rho) \quad (2)$$

$$G_{2q}(\rho) = \lim_{k_1 \longrightarrow 0} G_2(\rho) \quad (3)$$

and are as given in [1]. Next, we define the region of validity of the quasi-dynamic approximation G_{iq} by defining a quasi-dynamic radius (R_q) such that

$$\left|\frac{G_i(\rho) - G_{iq}(\rho)}{G_i(\rho)}\right| \leq \ error \ for \ all \ \rho \leq R_q \quad (4)$$

where *error* is any specified error tolerance.

2.1.2 The Asymptotic Approximation

In a similar fashion, the asymptotic approximations $G_{1a}(\rho)$ and $G_{2a}(\rho)$ for $G_1(\rho)$ and $G_2(\rho)$ are defined as

$$G_{1a}(\rho) = \lim_{\rho \longrightarrow \infty} G_1(\rho) \quad (5)$$

$$G_{2a}(\rho) = \lim_{\rho \longrightarrow \infty} G_2(\rho) \quad (6)$$

and though they are defined in the limiting sense as $\rho \longrightarrow \infty$, they are generally valid to an excellent accuracy for ρ greater than a fraction of a free space wavelength for most practical microstrip circuits [9]. In this paper, the asymptotic solution is obtained by deforming the path of integration in $G_1(\rho)$ and $G_2(\rho)$ to the path of steepest descent and using the first order approximation for the Hankel functions. Next, we define the region of validity of the asymptotic solution by an asymptotic radius R_a such that:

$$\left|\frac{G_i(\rho) - G_{ia}(\rho)}{G_i(\rho)}\right| \geq \ error \ for \ all \ \rho \geq R_a \quad (7)$$

Thus, in order to efficiently evaluate the moment method generalized impedance matrix, we first compute the quasi-dynamic radius R_q and the asymptotic radius R_a subject to a specified error tolerance. The Green's functions $G_1(\rho)$ and $G_2(\rho)$ are then evaluated using the quasi-dynamic solution for $\rho \leq R_q$, the dynamic solution for $R_q \leq \rho \leq R_a$, and finally the asymptotic solution for $\rho \geq R_a$. This is particularly useful in analyzing electrically large structures as most of the computations occur in the region ($\rho \geq R_a$). Once the numerical apparatus for computing the Green's of the problem has been laid out, the computation of the current distribution on the metallic structures is obtained using a standard Moment Method technique [1]. The extraction of the frequency dependent network parameters of arbitrary geometries has been fully described in [1]. Finally in order to validate this new approach, several examples have been solved and compared with available data and measurement. In this paper, we present the following example.

3 Computation of The [S] Parameters of a Tapered Two Conductor Transmission Line

In this example we solve for the [S] parameters of a tapered two conductor transmission line. The line geometrical and electrical data are shown in Fig. 2. A 4-port network is then defined by 4 reference planes 1.6 cms apart and symmetrically located from the port ends. The 3D frequency dependent [S] parameters are then extracted from the current distribution as described in [1]. In order to check the results, we approximate the line by a cascade of four uniform lines L1, L2, L3, and L4. The lines have different separations S1, S2, S3, and S4 (Fig. 2b). The length of each section is one fourth of the total length of the line (0.4 cms). The 2D frequency dependent [S] parameters of the of the line are then computed from the individual [S] parameters of each section using a 2D EFIE formulation [4 , 5 , 10] and standard network theory. The 3D and 2D S parameters have been computed at several frequencies. At 3, 4, and 5 Ghz, they are given in tables (1.1-1.3). It can be seen from these tables that the agreement between the 3D and 2D results is reasonable.

4 Conclusion

A new Dynamic approach, based on using near and far field approximations for the sommerfeld microstrip green's functions in the analysis of non-uniform microstrip transmission lines and discontinuities has been presented. The accuracy of these approximations can be set to any desired value. This is particularly useful in the analysis of electrically large circuits as it offers a significant reduction in the computational effort without sacrificing accuracy. Also, in this new approach, a substantial reduction in the moment method matrix size has been achieved by a proper choice of the basis functions for the current distribution on multiconductor transmission lines. Finally in order to check the accuracy of this new technique, several numerical examples have been solved and checked with available data and experiment.

5 REFERENCES

[1] Tawfik R. Arabi, Arthur T. Murphy, and Tapan K. Sarkar, "Electric Field Integral Equation Formulation For a Dynamic Analysis of Non-Uniform Microstrip Multi-Conductor Transmission Lines," **Accepted for publication in IEEE Trans. Microwave Theory**

Tech.

[2] Chalmers M. Butler, " The Equivalent Radius of a Narrow Conducting Strip," **IEEE Trans., Antennas Propagat.** , Vol. AP-30, No. 4, pp. 755-758, July 1982.

[3] M. Kobayashi, "Longitudinal and Transverse current distributions on microstrip lines and their closed-form expressions," **IEEE Trans. Microwave Theory Tech.** , Vol. MTT-33, pp. 952-959, Oct. 1985.

[4] Cao Wei, Roger F. Harrington, Joseph R. Mautz and Tapan K. Sarkar "Multiconductor Transmission Lines in Multilayered Dielectric Media," **IEEE Trans. Microwave Theory Tech.** , Vol. MTT-32, pp. 439-450, April 1984.

[5] T. R. Arabi, T. K. Sarkar, and A. R. Djordjevic "Time And Frequency Domain Characterization Of Multiconductor Transmission Lines," **Journal of Electromagnetics.** , Vol. 9 1989, pp. 85-112, Dec. 1989.

[6] M. Marin, S. Barkeshli, and P. H. Pathak, "On The Location of Proper and Improper Surface Wave Poles for The Grounded Dielectric slab," **IEEE Trans. Antennas Propagat.,** Vol. AP-38, pp. 570-573, April 1990.

[7] Chung-I G. Hsu, Roger F. Harrington, Joseph R. Mautz, and Tapan K. Sarkar, "On The Location of Leaky Wave Poles for a Grounded Dielectric Slab," **IEEE Trans., Microwave Theory Tech.,** Vol., MTT-39, pp. 346-349, Feb., 1991.

[8] J. R. Mosig and T. K. Sarkar, " Comparison of Quasi-Static and Exact Electromagnetic Fields From a Horizontal Electric Dipole Above a Lossy Dielectric Backed by an Imperfect Ground Plane," **IEEE Trans., Microwave Theory Tech.,** Vol., MTT-34, pp. 379-387, April 1986.

[9] Miguel Marin, Sina Barkeshli, and Prabhakar H. Pathak, "Efficient Analysis of Planar Microstrip Geometries Using a Closed-Form Asymptotic Representation of the Grounded Dielectric Slab Green's Function," **IEEE Trans., Microwave Theory Tech.** , Vol. MTT-37, pp. 669-679, April 1989.

[10] Antonije R. Djordjevic and Tapan K. Sarkar "Analysis Of Time Response of Lossy Multiconductor Transmission Line Networks," **IEEE Trans., Microwave Theory Tech.** , Vol. MTT-35, pp. 898-908, October 1987.

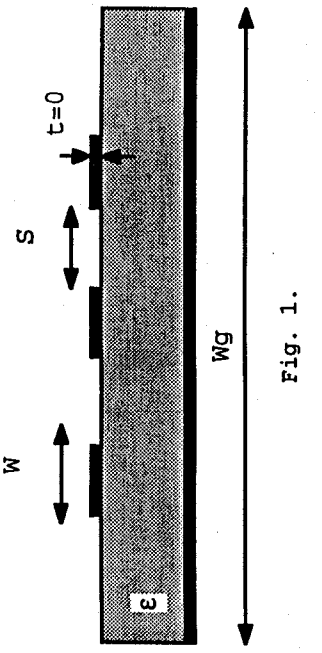

Fig. 1.

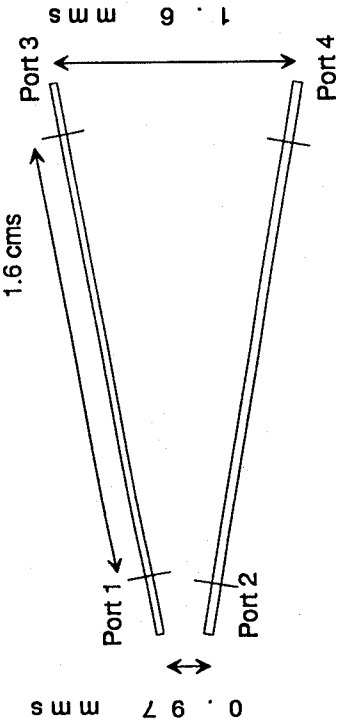

Fig. 2a

F = 3 GHz.

$$[S]^{3D}_{Mag} = \begin{bmatrix} 0.3671E-02 & 0.3018E-01 & 0.9669E+00 & 0.7642E-01 \\ 0.3018E-01 & 0.3671E-02 & 0.7642E-01 & 0.9669E+00 \\ 0.9663E+00 & 0.7623E-01 & 0.7253E-02 & 0.2925E-01 \\ 0.7623E-01 & 0.9663E+00 & 0.2925E-01 & 0.7253E-02 \end{bmatrix}$$

$$[S]^{2D}_{Mag} = \begin{bmatrix} 0.3317E-02 & 0.3890E-01 & 0.9646E+00 & 0.8874E-01 \\ 0.3890E-01 & 0.3318E-02 & 0.8874E-01 & 0.9646E+00 \\ 0.9646E+00 & 0.8874E-01 & 0.9832E-02 & 0.3705E-01 \\ 0.8874E-01 & 0.9646E+00 & 0.3705E-01 & 0.9833E-02 \end{bmatrix}$$

$$[S]^{3D}_{Pha} = \begin{bmatrix} 0.1204E+01 & -0.3442E+00 & -0.2625E+01 & 0.2061E+01 \\ -0.3442E+00 & 0.1204E+01 & 0.2061E+01 & -0.2625E+01 \\ -0.2625E+01 & 0.2082E+01 & 0.1302E+01 & -0.1717E+01 \\ 0.2082E+01 & -0.2625E+01 & -0.1717E+01 & 0.1302E+01 \end{bmatrix}$$

$$[S]^{2D}_{Pha} = \begin{bmatrix} 0.1786E+01 & -0.2130E+00 & -0.2649E+01 & 0.2047E+01 \\ -0.2130E+00 & 0.1786E+01 & 0.2047E+01 & -0.2649E+01 \\ -0.2649E+01 & 0.2047E+01 & 0.1492E+01 & -0.1891E+01 \\ 0.2047E+01 & -0.2649E+01 & -0.1891E+01 & 0.1492E+01 \end{bmatrix}$$

Table 1.1

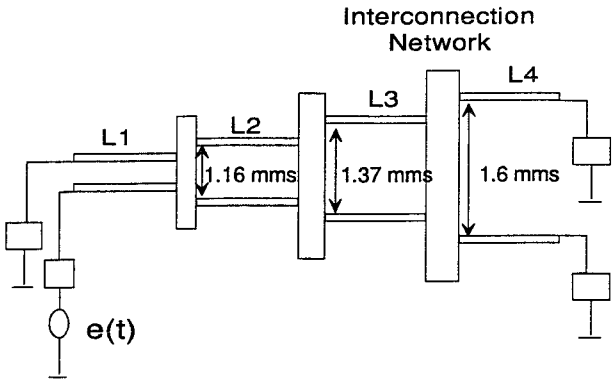

All terminations are 50 Ohms, All line lengths are 0.4 cms

Fig. 2b

F = 5 GHz

$$[S]^{3D}_{Mag} = \begin{bmatrix} 0.7048E-02 & 0.4577E-01 & 0.9470E+00 & 0.1086E+00 \\ 0.4577E-01 & 0.7048E-02 & 0.1086E+00 & 0.9470E+00 \\ 0.9449E+00 & 0.1079E+00 & 0.4056E-02 & 0.4367E-01 \\ 0.1079E+00 & 0.9449E+00 & 0.4367E-01 & 0.4056E-02 \end{bmatrix}$$

$$[S]^{2D}_{Mag} = \begin{bmatrix} 0.5580E-01 & 0.6218E-01 & 0.9386E+00 & 0.1406E+00 \\ 0.6218E-01 & 0.5581E-02 & 0.1406E+00 & 0.9386E+00 \\ 0.9386E+00 & 0.1406E+00 & 0.3419E-02 & 0.5839E-01 \\ 0.1406E+00 & 0.9386E+00 & 0.5839E-01 & 0.3418E-02 \end{bmatrix}$$

$$[S]^{3D}_{Pha} = \begin{bmatrix} 0.2067E+01 & 0.3745E+00 & 0.2043E+01 & 0.4678E+00 \\ 0.3745E+00 & 0.2067E+01 & 0.4678E+00 & 0.2043E+01 \\ 0.2044E+01 & 0.4681E+00 & 0.1846E+01 & 0.5530E+00 \\ 0.4681E+00 & 0.2044E+01 & 0.5530E+00 & 0.1846E+01 \end{bmatrix}$$

$$[S]^{2D}_{Pha} = \begin{bmatrix} 0.1934E+01 & 0.2880E+00 & 0.1987E+01 & 0.4032E+00 \\ 0.2880E+00 & 0.1934E+01 & 0.4032E+00 & 0.1987E+01 \\ 0.1987E+01 & 0.4032E+00 & -0.3218E+00 & 0.5316E+00 \\ 0.4031E+00 & 0.1987E+01 & 0.5317E+00 & -0.3224E+00 \end{bmatrix}$$

Table 1.3

F = 4 Ghz

$$[S]^{3D}_{Mag} = \begin{bmatrix} 0.7891E-02 & 0.2357E-01 & 0.9575E+00 & 0.9179E-01 \\ 0.2357E-01 & 0.7891E-02 & 0.9179E-01 & 0.9575E+00 \\ 0.9573E+00 & 0.9166E-01 & 0.1009E-01 & 0.2049E-01 \\ 0.9166E-01 & 0.9573E+00 & 0.2049E-01 & 0.1009E-01 \end{bmatrix}$$

$$[S]^{2D}_{Mag} = \begin{bmatrix} 0.5214E-02 & 0.3488E-01 & 0.9532E+00 & 0.1138E+00 \\ 0.3488E-01 & 0.5214E-02 & 0.1138E+00 & 0.9532E+00 \\ 0.9532E+00 & 0.1138E+00 & 0.9206E-02 & 0.3098E-01 \\ 0.1138E+00 & 0.9532E+00 & 0.3099E-01 & 0.9208E-02 \end{bmatrix}$$

$$[S]^{3D}_{Pha} = \begin{bmatrix} 0.1685E+01 & 0.5589E+00 & 0.2888E+01 & 0.1301E+01 \\ 0.5589E+00 & 0.1685E+01 & 0.1301E+01 & 0.2888E+01 \\ 0.2888E+01 & 0.1312E+01 & 0.1183E+01 & 0.2006E+01 \\ 0.1312E+01 & 0.2888E+01 & 0.2006E+01 & 0.1183E+01 \end{bmatrix}$$

$$[S]^{2D}_{Pha} = \begin{bmatrix} 0.2205E+01 & 0.4397E+00 & 0.2846E+01 & 0.1262E+01 \\ 0.4397E+01 & 0.2205E+01 & 0.1262E+01 & 0.2846E+01 \\ 0.2846E+01 & 0.1262E+01 & 0.9592E+01 & 0.2082E+01 \\ 0.1262E+01 & 0.2846E+01 & 0.2082E+01 & 0.9590E+00 \end{bmatrix}$$

Table 1.2